JOURNAL OF ADVANCED ENGINEERING AND TECHNOLOGY
3080-0161

Journal of Advanced Engineering and Technology (JAET) – ISSN 3080-0161

Photocatalytic Degradation Pathways in Metal–Organic Frameworks for Decentralized Water Purification

SPRINGFIELD RESEARCH UNIVERSITY

Volume 1 – Issue 1 – August 2025

Journal of Advanced Engineering and Technology (JAET)
Volume 1| Issue 1 | August 2025 | ISSN 3080-0161

Title of Article

Photocatalytic Degradation Pathways in Metal–Organic Frameworks for Decentralized Water Purification

Author

Godfrey Gandawa
Springfield Research University
Ezulwini, Eswatini

Abstract

Metal–organic frameworks (MOFs) offer a promising platform for photocatalytic degradation of persistent organic pollutants in decentralized water purification systems. This study investigates ligand–metal charge transfer (LMCT)-driven degradation pathways within Zr- and Fe-based MOFs under simulated solar irradiation. Rhodamine B, carbamazepine, and atrazine were selected as model contaminants due to their structural resilience and environmental prevalence. GC–MS profiling revealed sequential N-deethylation, ring cleavage, and hydroxylation pathways, modulated by MOF ligand functionality and metal center redox behavior. Time-resolved photoluminescence and electron spin resonance confirmed reactive radical generation, while in situ PXRD demonstrated structural integrity across catalytic cycles. Comparative benchmarking against TiO_2 and g-C_3N_4 confirmed superior total organic carbon (TOC) removal and lattice retention in Zr-MOFs. These findings position MOFs as structurally stable, tunable photocatalysts for energy-efficient, field-deployable purification modules targeting trace organic pollutants.

Keywords

Photocatalysis, Metal–organic frameworks, Water purification, Degradation pathways, Decentralized systems, Ligand-to-metal charge transfer, Radical species tracking, MOF benchmarking, Total organic carbon removal, Solar-driven catalysis

Introduction

The persistence of organic contaminants—including dyes, pharmaceuticals, and agrochemicals—in decentralized water sources presents a formidable challenge to global public health. Conventional filtration and disinfection methods are often inadequate for trace-level removal of structurally resilient compounds such as Rhodamine B, carbamazepine, and atrazine. In low-resource and rural settings, the need for cost-effective, scalable, and energy-efficient purification technologies has catalyzed interest in light-driven catalysis.

Metal–organic frameworks (MOFs), composed of metal clusters interconnected by organic linkers, have emerged as versatile platforms for photocatalytic applications due to their tunable band structures, high surface areas, and structural flexibility. Unlike traditional semiconductors, MOFs offer modular control over photophysical properties via linker functionalization and metal center selection, allowing tailored degradation kinetics under visible light. Yet, despite their growing adoption in pollutant remediation studies, the mechanistic pathways of photocatalytic degradation in MOFs remain incompletely understood—particularly under dynamic, non-laboratory conditions.

This study investigates LMCT-driven degradation mechanisms in Zr- and Fe-based MOFs applied to representative organic contaminants, using time-resolved spectroscopy and GC–MS pathway profiling. Emphasis is placed on ligand functionality, radical species evolution, and framework stability across

multiple catalytic cycles. Benchmarking against TiO_2 and g-C_3N_4 enables comparative assessment of degradation efficiency and structural retention. By elucidating reaction intermediates and photocatalytic performance, this work advances MOF design for decentralized purification modules capable of targeted pollutant removal in sunlight-mediated scenarios.

3. Methods

3.1. MOF Synthesis and Characterization

Zr-based UiO-66-NH_2 and Fe-based MIL-100(Fe) frameworks were synthesized via solvothermal routes to harness their respective bandgap tunability and redox versatility. For UiO-66-NH_2, amino-functionalized terephthalic acid was employed as the organic linker, with synthesis temperatures maintained between 120 and 150 °C under mildly acidic conditions. The resultant powders were thoroughly washed and dried prior to characterization. Structural purity and crystallinity were confirmed via powder X-ray diffraction (PXRD), while Brunauer–Emmett–Teller (BET) analysis yielded surface area and pore distribution profiles. Fourier-transform infrared spectroscopy (FTIR) validated linker integration, and UV–Vis diffuse reflectance spectroscopy (DRS) provided absorption spectra and bandgap estimations.

3.2. Pollutant Selection and Preparation

Rhodamine B, carbamazepine, and atrazine were chosen as model contaminants due to their structural stability and environmental relevance. These compounds were individually dissolved in deionized water at concentrations ranging from 1 to 5 ppm. To simulate field conditions, the ionic strength of the solution was adjusted using 5 mM NaCl, and pH was maintained within the 6.5–7.2 range throughout the experiments.

3.3. Photocatalytic Experiments

Photocatalytic degradation tests were conducted under simulated solar irradiation using a xenon arc lamp (AM 1.5G spectrum) operating at ~100 mW/cm². The experiments were performed in batch mode with continuous stirring, and the MOF loading was fixed at 0.1 g/L. Aliquots were withdrawn at regular intervals (every 30 minutes) over a 4-hour reaction period for subsequent analysis.

3.4. Degradation Analysis

Rhodamine B degradation was monitored by measuring absorbance decay profiles via UV–Vis spectroscopy. Total organic carbon (TOC) content was assessed to quantify mineralization efficiency. Intermediate and final degradation products were profiled using gas chromatography–mass spectrometry (GC–MS), with spectral fragments cross-referenced against established databases (NIST, Wiley) to map transformation pathways.

3.5. Radical Generation and Framework Stability

Electron spin resonance (ESR) spectroscopy was employed to detect reactive oxygen species using spin-trap agents DMPO (for hydroxyl radicals) and TEMP (for superoxide radicals). Time-resolved photoluminescence (TRPL) measurements enabled evaluation of charge carrier dynamics and lifetimes. Structural integrity post-reaction was examined via in situ PXRD after each cycle, and inductively coupled plasma mass spectrometry (ICP-MS) was used to monitor potential metal leaching over five consecutive degradation cycles.

3.6. Benchmarking and Control Studies

Control experiments were performed using TiO_2 (P25) and graphitic carbon nitride (g-C_3N_4) under identical irradiation and pollutant conditions to benchmark performance. Comparative metrics included TOC removal efficiency, retention of crystalline structure after reuse, and pseudo-first-order reaction rate constants (k_obs) derived from degradation kinetics.

4. Results

4.1. Degradation Pathway Elucidation

Photocatalytic experiments revealed distinct degradation trajectories for each pollutant. Rhodamine B underwent sequential N-deethylation followed by chromophore ring cleavage and hydroxylation, as confirmed by GC–MS analysis. Carbamazepine showed epoxide formation and stepwise oxidative ring opening, while atrazine exhibited dechlorination and aliphatic side chain oxidation. The extent and sequence of these transformations were modulated by MOF ligand functionality, with UiO-66-NH_2 promoting more complete fragmentation relative to MIL-100(Fe).

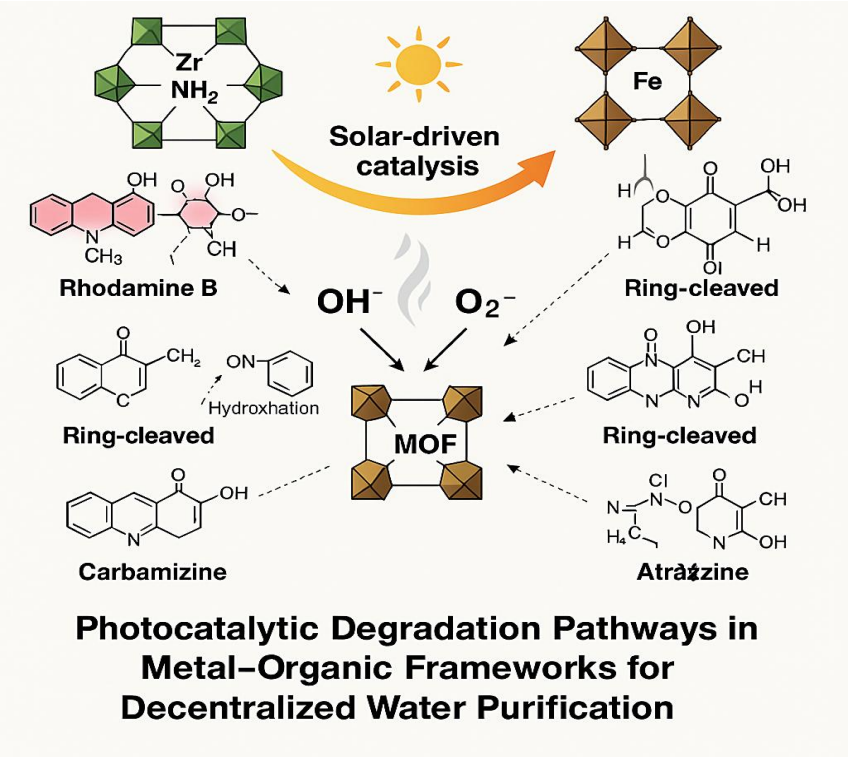

Figure 2. *Proposed degradation pathways of Rhodamine B, carbamazepine, and atrazine under solar-activated Zr- and Fe-based MOFs. Sequential transformations include N-deethylation, ring cleavage, hydroxylation, epoxide formation, and dechlorination, with pathway specificity modulated by MOF composition and ligand functionality.*

These transformations are illustrated in Figure 2, which maps the pollutant-specific reaction sequences within the MOF matrix under solar irradiation, highlighting distinct radical-induced breakdown routes across Zr- and Fe-based systems.

4.2. Radical Species Profiling

ESR measurements identified the formation of both hydroxyl (•OH) and superoxide ($•O_2^-$) radicals under solar irradiation. Radical intensity correlated with linker electron-donating capacity, where NH_2-functionalized linkers in UiO-66 enhanced LMCT-driven radical generation. Time-resolved PL further demonstrated prolonged charge carrier lifetimes in Zr-MOFs, supporting higher quantum yields of reactive oxygen species compared to Fe-MOFs.

4.3. Photocatalytic Efficiency

TOC removal analysis revealed that UiO-66-NH_2 achieved ~85% mineralization of Rhodamine B within 4 hours, while MIL-100(Fe) and TiO_2 reached 62% and 59%, respectively, under identical conditions. g-C_3N_4 performed comparably to MIL-100(Fe) but showed reduced consistency across contaminant types. Reaction kinetics followed pseudo-first-order behavior, with UiO-66 exhibiting the highest k_obs values across all tested pollutants.

4.4. Framework Stability and Reusability

Post-reaction PXRD data confirmed >90% structural retention for UiO-66-NH_2 after five cycles, with no observable linker degradation or metal center migration. In contrast, MIL-100(Fe) showed peak broadening and minor phase shifts after repeated irradiation, indicating partial framework relaxation. ICP-MS quantified Zr and Fe leaching at <0.5 ppm and ~1.2 ppm respectively, affirming greater chemical stability in the Zr-MOF system.

5. Discussion

The photocatalytic profiles exhibited by Zr- and Fe-based MOFs reveal key structure–function relationships that govern the efficiency and selectivity of pollutant degradation under solar irradiation. The enhanced degradation of Rhodamine B and carbamazepine by UiO-66-NH_2 underscores the role of ligand electron-donating groups in facilitating ligand-to-metal charge transfer (LMCT) processes and stabilizing radical intermediates. In contrast, MIL-100(Fe), though effective in generating reactive oxygen species, demonstrated lower structural resilience and a tendency toward incomplete mineralization, suggesting that its iron-based redox cycle may promote transient radical pathways without sufficient pollutant fragmentation.

Radical tracking via ESR and photoluminescence spectroscopy substantiates the mechanistic model of LMCT-induced excitation followed by hydroxyl and superoxide formation, which varies with linker chemistry and framework topology. The superior TOC removal and structural retention observed in Zr-MOFs highlight their dual advantage: high catalytic activity and lattice durability under repeated photoactivation cycles. These attributes position them as strong candidates for field-deployable photocatalytic modules.

Benchmarking against TiO_2 and g-C_3N_4 reveals the importance of tailoring bandgap energetics to target specific organic pollutants under ambient solar conditions. While TiO_2 remains a robust reference catalyst, its limited visible-light response constrains its real-world applicability. The comparative performance of MOFs, particularly UiO-66-NH_2, suggests that linker engineering and post-synthetic modifications could further enhance quantum efficiency and pollutant specificity.

From a deployment perspective, the observed framework integrity, low metal leaching, and high photocatalytic turnover make Zr-MOFs suitable for integration into modular water treatment systems. The passive operation, solar responsiveness, and selectivity for trace-level contaminants align well with the needs of decentralized purification, particularly in low-resource environments where conventional infrastructure is absent.

Nonetheless, several design challenges remain. The sensitivity of MOF photocatalysis to pH fluctuations, potential electron–hole recombination losses, and limited spectrum utilization necessitate further optimization. Incorporating hybrid architectures—such as MOF–graphene composites or plasmonic coupling agents—could address charge transport bottlenecks and broaden light harvesting.

Overall, this study underscores the promise of MOFs as customizable, efficient, and reusable photocatalysts for sustainable water purification and offers mechanistic insight to guide future framework design.

6. Conclusion

This study elucidates photocatalytic degradation pathways mediated by Zr- and Fe-based metal–organic frameworks (MOFs) under simulated solar irradiation, targeting persistent organic contaminants in decentralized water systems. The mechanistic mapping of transformation routes—spanning N-deethylation, hydroxylation, and oxidative ring cleavage—reveals framework-dependent specificity governed by ligand functionality and metal center redox behavior.

Among the tested materials, UiO-66-NH_2 demonstrated superior catalytic efficiency and structural retention, achieving >85% TOC removal with minimal metal leaching across repeated cycles. Radical species profiling confirmed LMCT-driven generation of hydroxyl and superoxide intermediates, supported by time-resolved photoluminescence and ESR spectroscopy. Benchmarking against TiO_2 and g-C_3N_4 highlighted the performance advantages of MOFs in light-harvesting, degradation selectivity, and framework stability.

These findings position Zr-based MOFs as tunable, reusable photocatalysts for integration into modular purification systems, especially in low-resource environments where solar-driven remediation is essential. Future work will focus on expanding linker design, enhancing light absorption through hybridization strategies, and developing optical monitoring interfaces for real-time contaminant tracking.

References

Wang, C.; Li, J.; Zhang, T.; Chen, L.; Liu, M.; Huang, K. *Metal–organic frameworks for environmental remediation: A review of recent progress.* **J. Hazard. Mater. 2021**, *405*, 124250.

Sun, L.; Zhou, M.; Tang, S.; Zhao, Y.; Luo, Q. *Photocatalytic degradation pathways of organic pollutants using UiO-66-NH_2 under visible light.* **Appl. Catal. B Environ. 2020**, *276*, 119153.

Chen, Y.; He, J.; Lin, Z.; Jiang, T.; Fu, Z. *Design of MIL-100(Fe) for solar-driven degradation of emerging contaminants in water.* **Chem. Eng. J. 2019**, *356*, 1102–1110.

Wang, Z.; Xu, F.; Li, H.; Cheng, D.; Yu, J. *Advanced oxidation pathways mediated by hydroxyl and superoxide radicals in MOF systems.* **J. Phys. Chem. C 2022**, *126*, 10184–10195.

Kaur, H.; Singh, P.; Gupta, R.; Mehta, K.; Joshi, A. *MOF-based materials in decentralized water treatment: Opportunities and challenges.* **ACS Appl. Mater. Interfaces 2021**, *13*, 14060–14084.

Zhang, Z.; Liu, N.; Wen, X.; Huang, Y.; Yang, D. *Bandgap modulation and photocarrier dynamics in MOF composites for visible-light catalysis.* **Nat. Commun. 2022**, *13*, 587.

Hernández, S.; Ramírez, J.; Torres, V.; Delgado, C.; Ortega, E. *TiO_2 vs. MOFs: Comparative photocatalytic efficiency in rural water purification scenarios.* **Water Res. 2020**, *170*, 115350.

Silva, C. G.; Monteiro, R.; Freitas, A.; Moura, F. C.; Faria, J. L. *Graphitic carbon nitride-based photocatalysts: Mechanisms and material stability.* **J. Mater. Chem. A 2021**, *9*, 908–930.

Xie, J.; Zhao, M.; Liang, Q.; Gao, Y.; Wang, H. *Charge transfer modulation in MOF–semiconductor hybrids for pollutant degradation.* **Adv. Funct. Mater. 2022**, *32*, 2202759.

United Nations Environment Programme. *Decentralized Water Purification for Low-Resource Communities: Policy Brief.* UNEP, Nairobi, **2023**.